Research Article

Juan Carlos Marín and Alberto Barroso*

Comparison of the shear behavior in graphite-epoxy composites evaluated by means of biaxial test and off-axis tension test

https://doi.org/10.1515/secm-2021-0022
received November 10, 2020; accepted January 12, 2021

Abstract: Characterization of shear behavior in composite materials remains a not fully solved problem. In the last fifty years, many different approaches have been proposed to solve this problem (rail shear, thin-walled tube torsion, off-axis tensile, ±45° tensile, Arcan, Iosipescu, asymmetric four-point bend, plate twist, v-notched rail shear, off-axis flexural, and shear frame), although none of these approaches have achieved an unquestionable solution. For this reason, proposals of alternative methods and comparison between different experimental techniques are of interest. In the present work, the use of cruciform samples with the fiber oriented at 45° with respect to the load directions, and subjected to tension-compression (creating a pure shear stress state at the central part of the samples), is studied. The experimental results of the cruciform samples have been compared with the off-axis tests (with the fiber at 10°) for the same material (AS4/8552), finding a good agreement between the shear experimental curves, especially at the initial part of the curve, where the shear modulus is calculated. Nevertheless, the shear strength value obtained by means of the cruciform specimen has shown to be significantly lower than that obtained using the off-axis test. A Finite Element numerical model of the cruciform specimen has been developed to analyze the stress field of the samples. Numerical results have shown that there is a central area of the cruciform specimens where a pure and uniform shear stress state is developed, which is suitable for the evaluation of the shear constitutive law of the material. It has been observed that there is a (σ_{22}) stress concentration in the transition between the straight and curved parts of the boundary geometry of the samples, which explain some premature failures of the samples. This premature failure could be avoided with tabs extended up to the beginning of the central part of the sample.

Keywords: composite materials, testing, off axis, cruciform samples, mechanical characterization

1 Introduction

The precise mechanical characterization of composite materials is a basic step for the design of structures made with these materials. In particular, the characterization of the shear behavior in composite materials still remains being a not fully solved problem. In the last fifty years, many different approaches have been proposed to solve this problem (rail shear, thin-walled tube torsion, off-axis tensile ±45° tensile, Arcan, Iosipescu, asymmetric four-point bend, plate twist, v-notched rail shear, off-axis flexural, and shear frame), although none of these approaches have achieved an unquestionable solution. For this reason, the proposal of new test methods and the comparison of the results with existing available procedures are of unquestionable interest.

The basic idea beyond the shear characterization tests is to generate a pure and uniform shear stress state in the area of the sample where measurements are being carried out, in order to directly obtain the shear modulus G_{12} and the shear strength S. It is well-known that a tension and a perpendicular and equal valued compression stress state are equivalent to a pure shear stress state at 45°. A way to produce a tension-compression loading state is by using cruciform specimens in biaxial loading testing machines [1–5]. The idea to use biaxial tests to obtain shear properties appears, for example, in Kennedy et al. [6], but using laminates $[90/0]_{2s}$ and $[\pm 45]_{2s}$. In the present work, the use of cruciform specimens, with carbon-epoxy unidirectional laminates at 45° with respect to

* **Corresponding author: Alberto Barroso,** Group of Elasticity and Strength of Materials, School of Engineering, University of Seville, Camino de los Descubrimientos s/n, 41092 Seville, Spain, e-mail: abc@us.es
Juan Carlos Marín: Group of Elasticity and Strength of Materials, School of Engineering, University of Seville, Camino de los Descubrimientos s/n, 41092 Seville, Spain

the loading directions, and subjected to a tension-compression loading state in a biaxial testing machine, is analyzed.

Experimental results obtained with the cruciform specimens will be compared (in terms of stiffness and strength values) with the 10° off-axis tension tests for the same material [7]. The off-axis test is a widely accepted test configuration for the shear characterization of composite materials due to its simplicity, as illustrated by the extensive literature devoted to its study and applications [8–21]. For this reason, the off-axis test has been selected as the reference configuration to compare with. In particular, the oblique tabs configuration [18] has been used in the off-axis test, as its efficiency has been demonstrated in previous works [7,22]. Nevertheless, the off-axis tension test does not produce a pure shear stress state, unlike the biaxial tension-compression test with cruciform samples.

2 Material and test coupons preparation

A graphite-epoxy composite denominated AS4/8552 and manufactured by HEXCEL Composites has been used in the present work. This material is the same as the one used in the off-axis tests which will be taken as reference values to compare with [7]. A rectangular panel 500 × 300 mm^2 has been manufactured using 4 plies of unidirectional pre-preg at 0°, giving rise to a final thickness of the cured panel of 0.85 ± 0.02 mm. The panel has been cured in an autoclave, using a vacuum bag, at 180°C and 7 bar. From this panel, cruciform specimens were obtained at 45° as schematically shown in Figure 1.

The test coupons were first cut using a diamond disc and were finally machined to get the final geometry (depicted in Figure 2), using a milling drill.

The dimensions were selected in accordance with the characteristics of the biaxial testing machine used in the tests. The arm ends of the samples were reinforced with tabs made of a glass fiber laminate to avoid premature failures at the machine jaw grips. The tabs were bonded using an adhesive curing at 180°C (SAFRAN). The final configuration of the cruciform specimens is shown in Figure 3.

3 Experimental tests

Tests were carried out in a biaxial testing machine (Figure 4a), with mechanical jaw grips (Figure 4b), and with independent load cells at each loading arm. Longitudinal and transversal displacements were measured using an optical video-extensometer. Figure 4b shows the white lines (horizontal and vertical) in the central part of the samples, used as a reference for the displacement measurements with the video-extensometer. Room temperature and relative humidity during the tests were 22°C and 50%, respectively. All tests have been carried out with control in force, using a loading rate of 10 N/s.

Figure 1: Cruciform specimens in the manufactured panel.

Each one of the tests was loaded until complete failure, with the tension load along the vertical axis and the compression applied along the horizontal direction. Figure 5 shows, for one of the tested samples (sample #2), (a) the initial stage of the test, and (b) the final stage, with the failure of the specimen. Although a

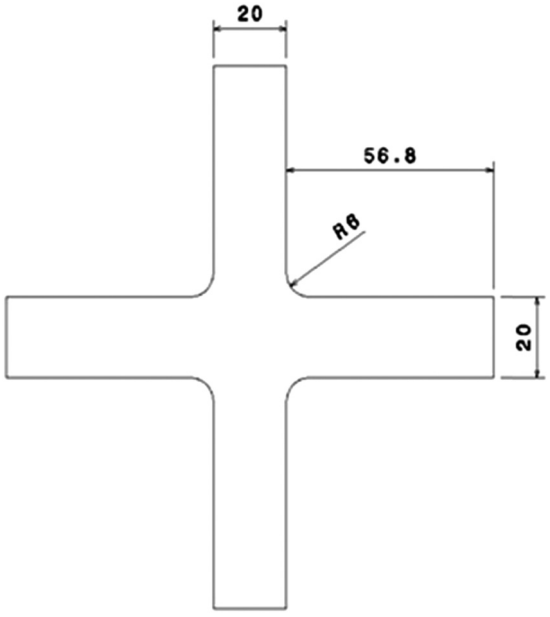

Figure 2: Sample's geometry and dimensions (in mm).

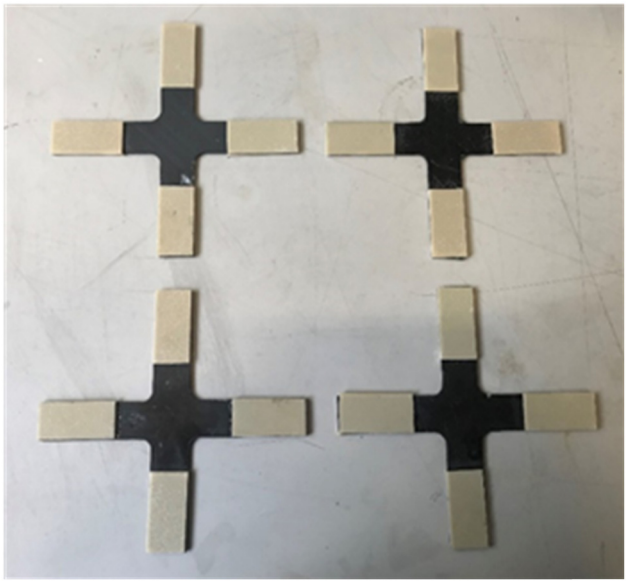

Figure 3: Cruciform samples ready to be tested.

detailed description of the failures will be given later, in Figure 5b failure initiates at the transition between the straight and the curved part of the sample, where some stress concentration appears, as it will be discussed later, in the numerical part of the work.

From each one of the tests, loading values for each loading arm, as well as the vertical and horizontal elongations of the white marks at the central area of the sample, were recorded. Figure 6 shows the absolute longitudinal normal stress at each loading arm vs the absolute value of the longitudinal normal strain associated to the compression loading arm. It can be observed that the values for the tensile loading direction are approximately equal to those associated to the compression loading direction, which guarantees the desired pure shear stress state at the central area of the sample.

From the measured longitudinal normal stresses, the shear stress σ_{12} in the orthotropic axis of the material (45° with respect to the loading arm directions) is directly obtained. The shear strain in orthotropic axis can be also easily obtained by simple subtraction of the vertical (ε_y) and horizontal (ε_x) longitudinal normal strains.

$$\gamma_{12} = \varepsilon_y - \varepsilon_x \tag{1}$$

Figure 7 shows σ_{12} vs γ_{12} obtained from the tests of samples 3, 4, 5, 6, and 7. Results for sample 2 could not be used, due to a failure with the recording of the video-extensometer device, and sample 1 broke while clamping it to the machine jaws. An initial linear behavior can be observed in the plots in Figure 7, which allows the measurement of the shear modulus G_{12} of the material. After this initial linear behavior, the typical nonlineal behavior associated to this materials tested in shear is observed, with higher dispersion than in the linear part of the curves. Finally, a more horizontal behavior is developed, associated to the final failure process of the samples. Table 1 shows the shear modulus values G_{12} measured using the initial linear part of the curves, together with the average value as well as the standard deviation.

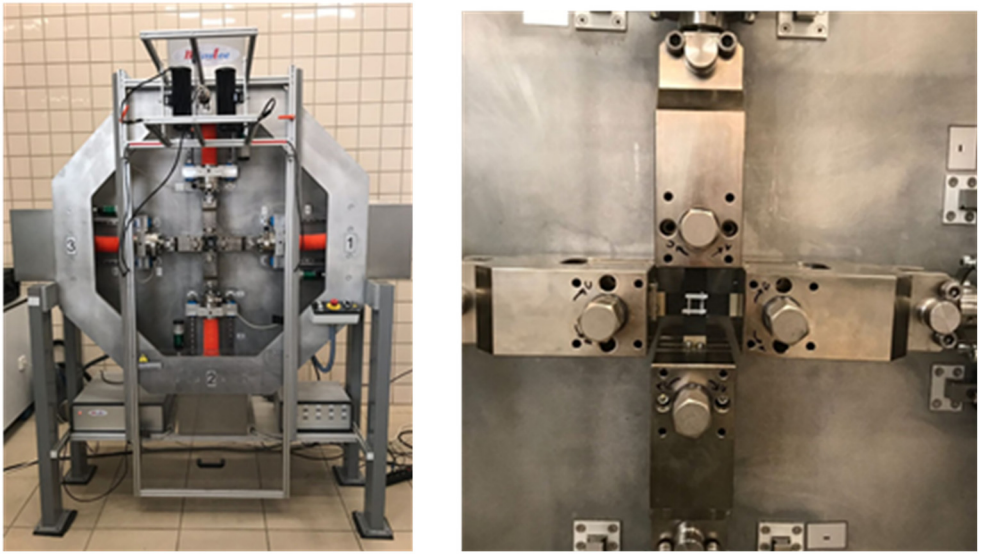

(a) (b)

Figure 4: Biaxial testing machine: (a) general view, (b) detail of the gripping system.

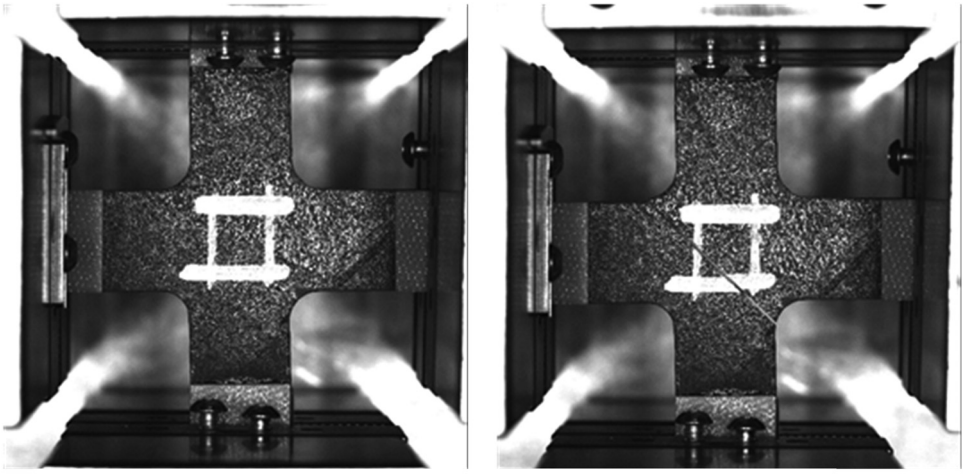

Figure 5: (a) Initial and (b) final stage of the biaxial test of sample #2.

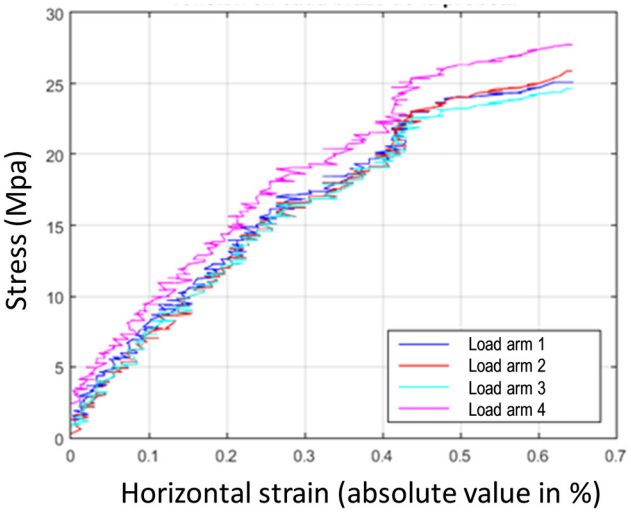

Figure 6: Example of the absolute values of the longitudinal normal stresses vs absolute value of the horizontal compression strain for a particular test.

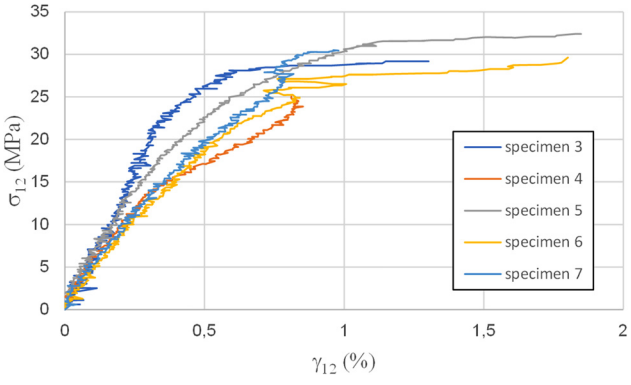

Figure 7: Experimental curves (σ_{12} vs γ_{12}) for samples 3–6.

Shear strength values for each sample are simply obtained as the value of the shear stress (σ_{12}) at the instant of failure. Table 2 shows the strength values ($S = \sigma_{12\_max}$) for each specimen, together with the average as well as the standard deviation.

Figure 8 shows the failures of all the tested specimens, all failures having in common the transition point from the straight loading arms and the curve part of the specimen and the failure along the central part of the sample. In particular, samples 3 and 5 exhibited a second failure, parallel to the initial failure plane, probably motivated by the dynamic effects of the first failure. No buckling effects have been observed in the horizontal (compression) arms.

Samples 3 and 5 (in Figure 8) have the same failure mode than the rest of samples. In the particular case of sample 3, there is a simultaneous failure at both stress concentration points (top-right and bottom-left) of the simple. In the case of sample 5, the energy released after the first failure, combined with the extremely brittle behavior of the samples, has made part of the sample to fall completely from the coupon. That is the reason why part of the sample does not appear in the Figure 8.

4 Results analysis

In order to check the suitability of the biaxial tension-compression test using cruciform specimens, results for the shear modulus and shear strength will be compared with experimental results obtained using the off-axis test (10°) with oblique tabs for the same material system

Table 1: Experimental measured values of the shear modulus G_{12}

Specimen number	3	4	5	6	7	Average value	STD
G_{12} (GPa)	5.393	4.747	5.347	4.224	4.512	4.845	0.514

Table 2: Experimental shear strength values for the tested samples

Specimen number	2	3	4	5	6	7	Average value	STD
σ_{12_max} (MPa)	26.756	28.462	25.050	31.554	25.234	27.700	27.459	2.412

(AS4/8552) [7]. Figure 9 shows the experimental curves σ_{12} vs γ_{12} from both the biaxial tests (in blue) and off-axis tests (in red). In the initial part of the curves, both test configurations show a similar linear behavior, with higher dispersion for the biaxial configuration and slightly higher values of the shear modulus for the biaxial configuration (G_{12} = 4.845 GPa) compared to the results for the off-axis 10° configuration (G_{12} = 4.423 GPa). For higher stress values, the dispersion of the curves increases for both test configurations, being more apparent for the biaxial test configuration, fact that the authors associate to the strain measurements carried out with the video-extensometer.

The shear strength values obtained with the biaxial test and the cruciform specimens are much lower than those obtained with the 10° off-axis tension test, as can be clearly observed in Figure 10.

The extremely brittle nature of failure in this type of samples makes the test results (a) to have a high sensitivity to local stress concentrations appearing in the sample geometry, and in consequence, (b) to have a

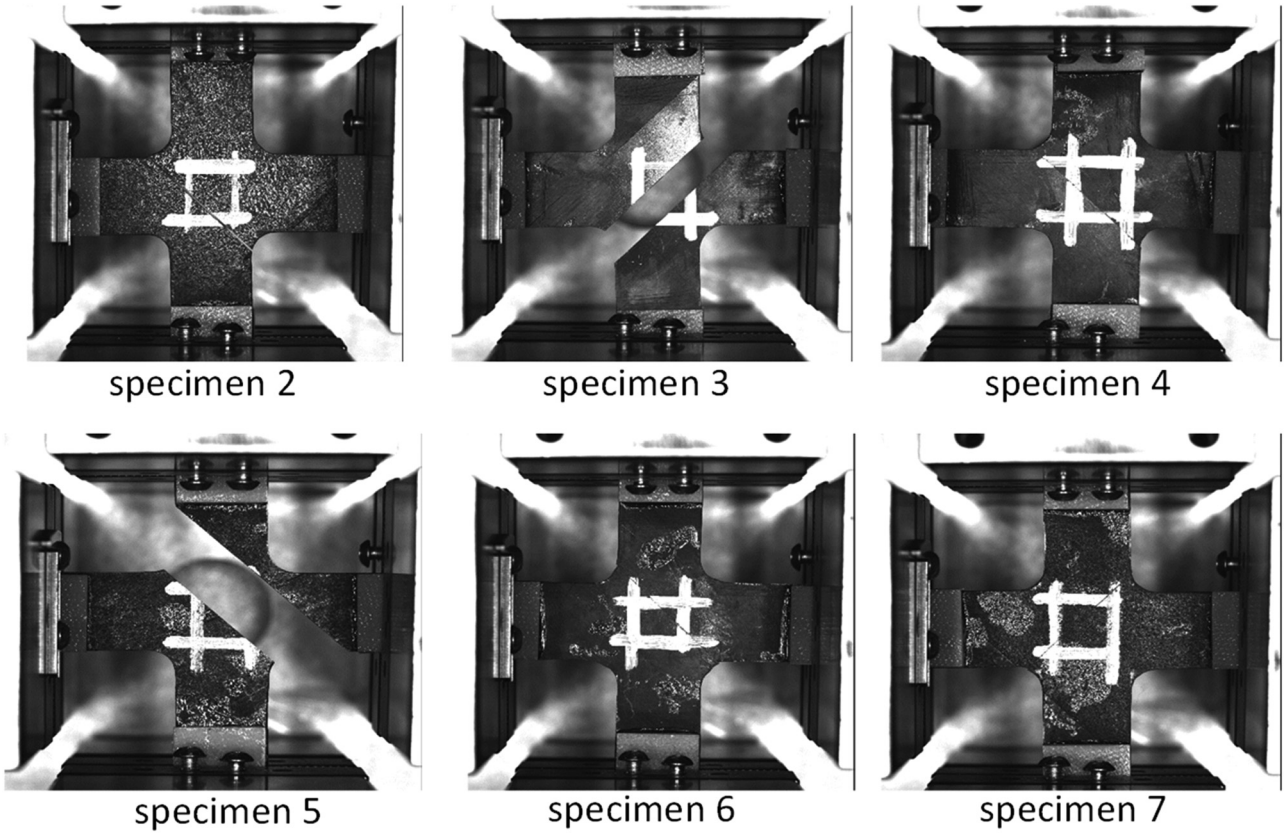

Figure 8: Failures of the biaxial test samples.

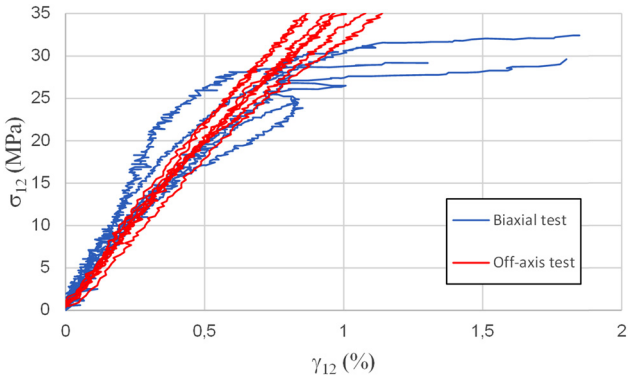

Figure 9: Comparison of the shear tests curves, for the evaluation of the shear modulus (G_{12}) using the biaxial test with cruciform specimens and the off-axis 10° test.

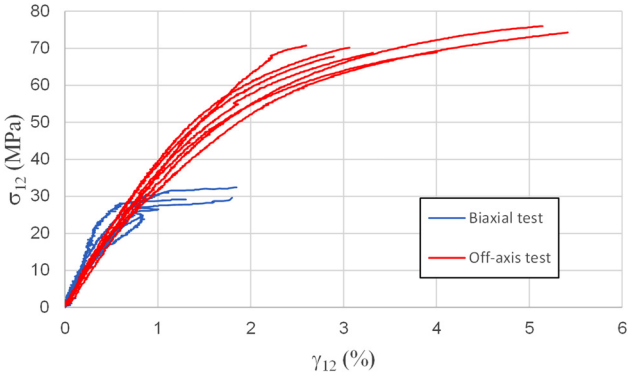

Figure 10: Comparison of the shear tests curves, for the evaluation of the shear strength (σ_{12_max}) for both test configurations.

higher dispersion in the strength results (as shown in Figure 9) when compared to other test procedures (off axis).

This fact indicates that the stress values at the instant of failure cannot be associated to the shear strength of the material, and that there must be a premature failure not associated with the shear stress state in the central part of the specimen. In order to try to corroborate this, a Finite Element model of the cruciform specimen under biaxial loading has been developed.

The numerical model was done with the commercial Finite Element code ANSYS 19.0, using SHELL63 elements, with 4 nodes and 6 degrees of freedom per node. Figure 11 shows the mesh of the model. Displacement boundary conditions were prescribed at the arm ends of the cruciform geometry, with equal values, positive (elongation) in the vertical arms and negative (contraction) in the horizontal arms. In the horizontal (vertical) arms, vertical (horizontal) displacements have been prescribed to simulate the gripping system of the testing

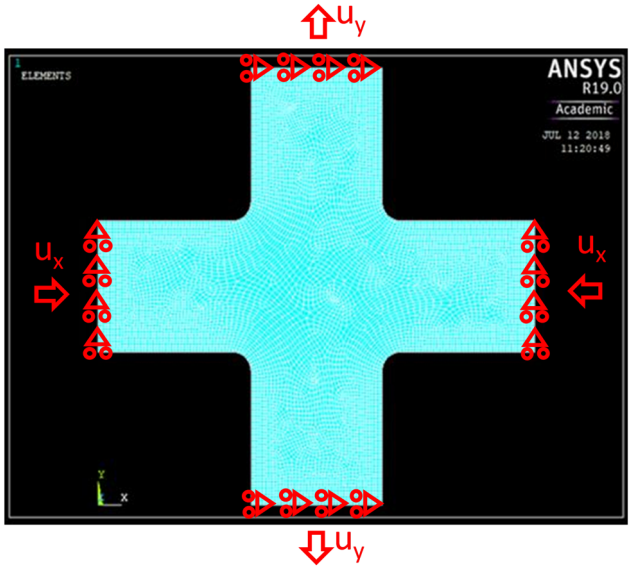

Figure 11: Finite element mesh of the model.

machine (Figure 11). Mechanical properties of the material were taken from reference [7]: E_{11} = 125.159 GPa, E_{22} = 8.112 GPa, G_{12} = 4.423 GPa, ν_{12} = 0.3.

Figures 12–14 show the contour plots of the (σ_{12}, σ_{11}, and σ_{22}) stress components, respectively. In Figure 12, a reasonable uniform shear stress state is observed at the central part of the specimen, and the measurements therein can be, then, reasonably well-related to the shear behavior of the material, in terms of stiffness.

In terms of the shear strength behavior, Figure 14 shows σ_{22} concentrations at the transition area between the straight and the curved part of the specimen boundary (at the central part of the coupon). This stress concentration

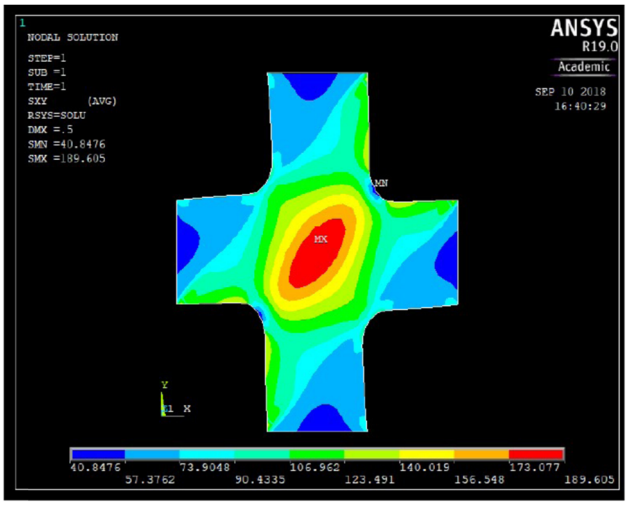

Figure 12: σ_{12} contour plot in the cruciform coupon.

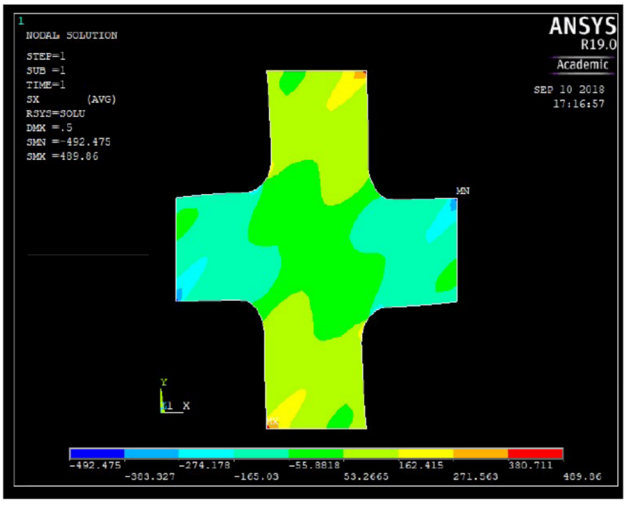

Figure 13: σ_{11} contour plot in the cruciform coupon.

seems to be responsible for the observed premature failure in the experimental tests, location where the tensile strength perpendicular to the fiber direction (Y_t) is reached. This strength value (Y_t) is significantly lower than the shear strength (S). In the same line, failure locations coincide, at the boundaries of the samples, with this transition zone, as can be observed in Figure 8. Two potential solutions alternatives, see ref. [23], to allow the use of these specimens for reliable strength measurements would be: (a) to use longer tabs, reaching almost the central part of the specimen, or (b) to use double curvature specimens to diminish the σ_{22} stress concentrations at the specimen boundaries and allow the failure to be initiated by the shear stress component σ_{12} at the central part of the sample. In any case, both alternatives make the preparation of the sample more difficult.

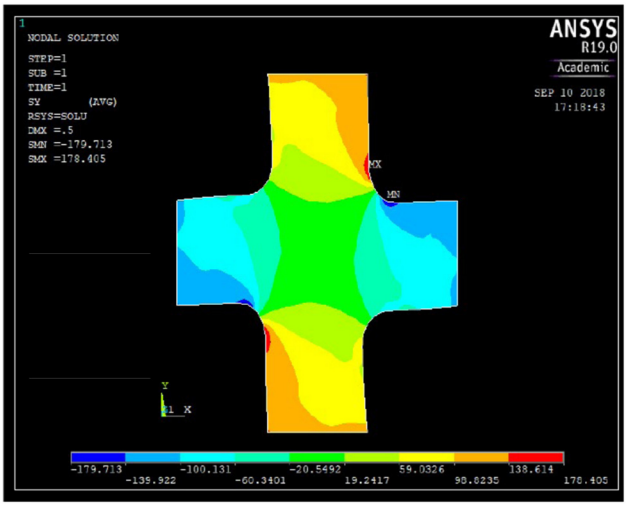

Figure 14: σ_{22} contour plot in the cruciform coupon.

5 Conclusion

In the present work, graphite-epoxy (AS4/8552) cruciform coupons (with the fiber oriented at 45° with respect to the loading directions) have been used to obtain the mechanical properties in shear (stiffness and strength), by means of a biaxial tension-compression test. The specimens have been machined from a unidirectional laminate, with the coupon geometry oriented at 45° with respect to the fiber direction. Biaxial tension-compression tests have been carried out to experimentally obtain the σ_{12} vs γ_{12} curves. Experimental results have been compared with the results for the same material obtained by the standard 10° off-axis tension test, finding a good agreement between both procedures in the initial part of the curves where the shear modulus is obtained, although it seems that the use of mechanical extensometers gives lower dispersion values when compared with the results using the video-extensometer. Nevertheless, strength values obtained with the cruciform specimen show to be much lower than those obtained with the 10° off-axis tension test. The brittle behavior of the material together with the presence of some local stress concentrations in the cruciform specimens has made some premature failures to appear which has affected the strength results. To analyze these observations, a numerical Finite Element model for the biaxial configuration has been developed. Numerical results confirm the existence of a pure and uniform shear stress state at the central part of the sample which allows the stiffness characterization to be performed with this test configuration. The concentration of the σ_{22} stress component has also been observed, which would justify the premature failure observed in the specimens. Thus, the use of the cruciform specimen is adequate for the shear modulus determination as it provides a better scenario for the shear measurement under study (pure shear and uniform state in the central part of the sample), but needs some geometrical modifications (tab reinforcements, or double curvature) to allow the strength measurements to be carried out in a reliable way.

With the experimental evidences observed in the present work, the biaxial test configuration is a suitable test configuration to characterize the shear behavior in composite materials, due to the fact that a pure and uniform shear stress state is produced in the central part of the sample, where measurements are carried out. The problems

associated with the premature failure of the samples when obtaining the shear strength of the material seem to be easily solvable by a simple modification of the geometry of the reinforcement tabs.

It is expected that once these premature failures are avoided, the shear strength values would correspond to a more realistic strength value of the material, as it is produced in a pure shear stress state.

Acknowledgments: This research was supported by the Spanish Ministry of Education, Culture and Sports (Project MAT2016-80879-P).

Conflict of interest: Authors state no conflict of interest.

References

1 Welsh JS, Mayes JS, Key CT, McLaughlin RN. Comparison of MCT failure prediction techniques and experimental verification for biaxially loaded gass fabric-reinforced composite laminates. J Comp Mat. 2004;38(24):2165–81.
2 Smits A, Van Hemelrijck D, Philippidis TP, Cardon A. Design of a cruciform specimen for biaxial testing of fibre reinforced composite laminates. Comp Sci Tech. 2006;66(7–8):964–75.
3 Ramault C, Makris A, Van Hemelrijck D, Lamkanfi E, Van Paepegem W. Comparison of different techniques for strain monitoring of a biaxially loaded cruciform specimen. Strain. 2011;47(SUPPL.2):210–7.
4 Vankan WJ, Tijs BHAH, Jong GJ, De Fred HC, Singh NK. Stregth of notched and un-notched thermoplastic composite laminate in biaxial tension and compression. J Comp Mat. 2016;50(25):3477–500.
5 Kobeissi A, Rahme P, Leotoing L, Guines D. Strength characterization of glass/epoxy plain weave composite under different biaxial loading ratios. J Comp Mat. 2020;54(19):2549–63.
6 Kennedy JM, Barnett TR, Farley GL. Experimental and analytical evaluation of a biaxial test for determining in-plane shear properties of composites. SAMPE Quat. 1992;27(1):28–37.
7 Marín JC, Justo J, Barroso A, Cañas J, París F. On the optimal choice of fibre orientation angle in off-axis tensile test using oblique end-tabs: theoretical and experimental studies. Comp Sci Tech. 2019;178:11–25.
8 Pagano NJ, Halpin JC. Influence of end constraint in the testing of anisotropic bodies. J Compos Mater. 1968;2(1):18–31.
9 Wu EM, Thomas RL. Off-axis test of a composite. J Compos Mater. 1968;2(4):523–6.
10 Rizzo RR. More on the influence of end constraint on off-axis tensile test. J Compos Mater. 1969;3:202–19.
11 Richards GL, Airhart TP, Ashton JE. Off-axis tensile coupon testing. J Compos Mater. 1969;3:586–9.
12 Pipes RB, Cole BW. On the off-axis strength test for anisotropic materials. J Compos Mater. 1973;7:246–56.
13 Chamis CC, Sinclair JH. Ten-deg off-axis test for shear properties in fiber composites. Exp Mech. 1977;17(9):339–46.
14 Chang BW, Huang PH, Smith DG. A pinned-end fixture for off-axis testing. Exp Tech. 1984;8(6):28–30.
15 Pindera MJ, Herakovich CT. Shear characterization of unidirectional composites with the off-axis tension test. Exp Mech. 1986;26(1):103–12.
16 Cron SM, Palazotto AN, Sandhu RS. The improvement of end-boundary conditions for off-axis tension specimen use. Exp Mech. 1988;28(1):14–9.
17 Sun CT, Berreth SP. A new end tab design for off-axis tension test of composite materials. J Compos Mater. 1988;22(8):766–79.
18 Sun CT, Chung I. An oblique end-tab design for testing off-axis composite specimens. Composites. 1993;24(8):619–23.
19 Marín JC, Cañas J, París F, Morton J. Determination of G_{12} by means of the off-axis tension test. Part I: review of gripping systems and correction factors. Compos Part A Appl Sci Manuf. 2002;33(1):87–100.
20 Marín JC, Cañas J, París F, Morton J. Determination of G_{12} by means of the off-axis tension test. Part II: a self-consistent approach to the application of correction factors. Compos Part A Appl Sci Manuf. 2002;33(1):101–11.
21 Xiao Y, Kawai M, Hatta H. An integrated method for off-axis tension and compression testing of unidirectional composites. J Compos Mater. 2011;45(6):657–69.
22 Barroso A, Marín JC, Mantič V, París F. Premature failures in standard test specimens with composite materials induced by stress singularities in adhesive joints. Int J Adhes Adhes. 2020;97:102478.
23 Correa E, Barroso A, Pérez MD, París F. Design for a cruciform coupon used for tensile biaxial transverse test son composite materials. Compos Sci Technol. 2017;145:138–48.